Supporting Information

Injectable Non-leaching Tissue-mimetic Bottlebrush Elastomers: A New Platform for Advancing Reconstructive Surgery

Erfan Dashtimoghadam[1], Farahnaz Fahimipour[1], Andrew N. Keith[1], Foad Vashahi[1], Pavel Popryadukhin[2], Mohammad Vatankhah-Varnosfaderani[1], Sergei S. Sheiko[1*]

[1]*Department of Chemistry, University of North Carolina at Chapel Hill, 27599, USA*

[2]*Instituteof Macromolecular Compounds of the Russian Academy of Sciences, St.Petersburg, Russia*

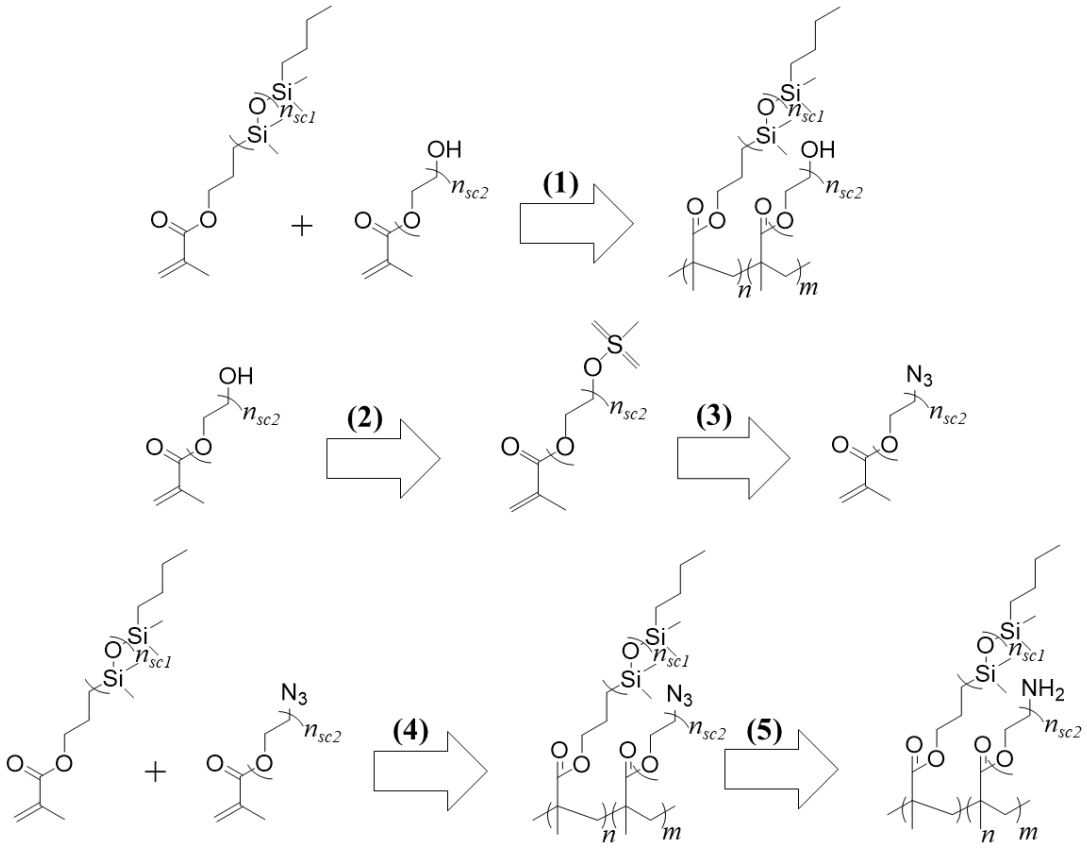

Figure S1. Synthesis of functional bottlebrush polymers and macromonomers: **(1)** synthesis of random polydimethylsiloxane-poly(ethylene glycol) bottlebrush copolymer (PDMS-*r*-PEG) through controlled radical copolymerization of polydimethylsiloxane-methacrylate (PDMSMA) and polyethyleneglycol-methacrylate (PEGMA) macromonomers, **(2)** mesylation of PEGMA macromonomer, **(3)** synthesis of azide-terminated PEGMA from mesylated macromonomer, **(4)** synthesis of random polydimethylsiloxane/azide-terminated poly(ethylene glycol) (PDMS-*r*-PEG.N_3) bottlebrush copolymer, and **(5)** reduction of PDMS-*r*-PEG.N_3 to achieve PDMS-*r*-PEG.NH_2 bottlebrush copolymer (for details of illustrated reactions, please see Methods Section).

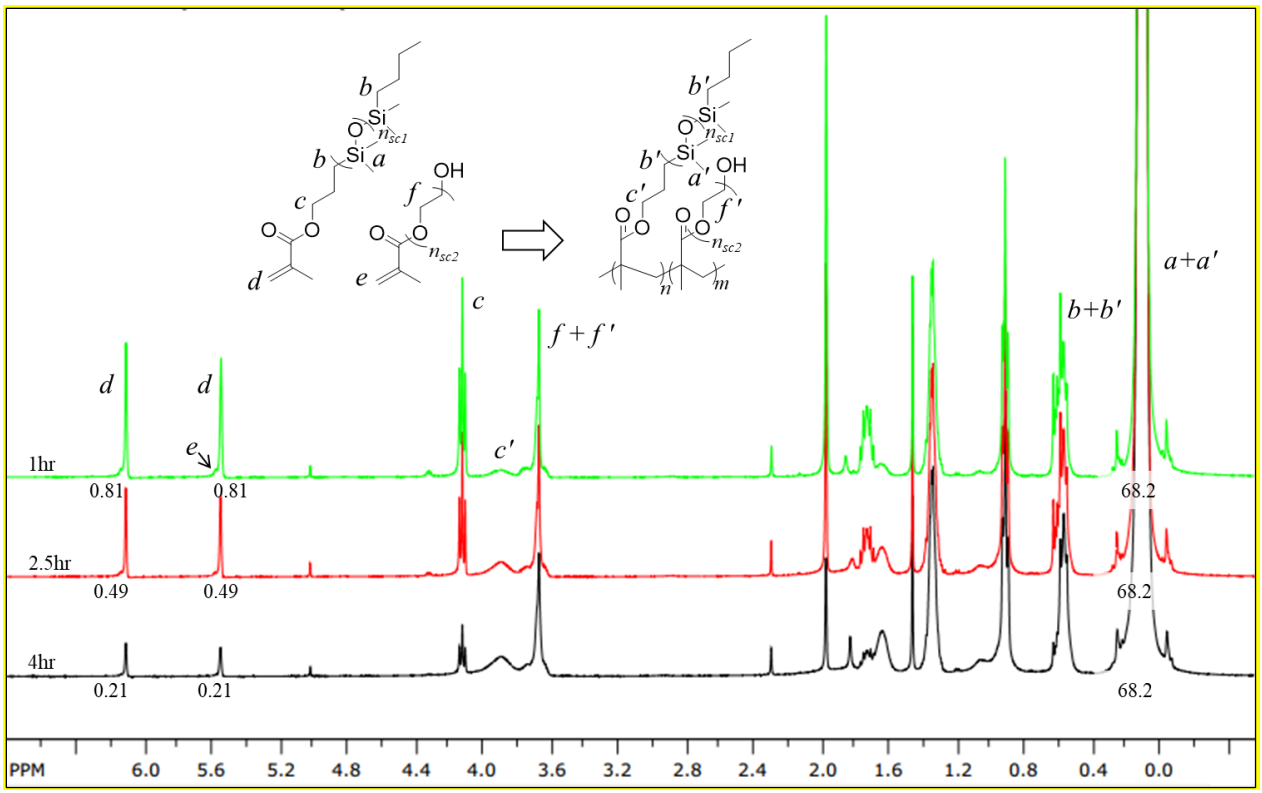

Figure S2. ^{1}H-NMR growth of a random polydimethylsiloxane-poly(ethylene glycol) brush (PDMS-*r*-PEG, *n*:*m*, 95:5, n_{sc1}: 14, n_{sc2}: 12) (400 MHz, $CDCl_3$): 6.16, 5.57 ($C\mathbf{H}_2$=C(CH_3)C=O, PDMS and PEG macromonomer mixture, s, 1H), 4.12 (CO-O$C\mathbf{H}_2$-, PDMS macromonomer, t, 2H), 3.91 (CO-O$C\mathbf{H}_2$-, PDMS brush, t, 2H), 3.78 (CO-O$C\mathbf{H}_2$-, PEG brush, t, 2H), 3.67 (-$OC_2\mathbf{H}_4$O-, PEG brush, m, 32H), 0.55 (-CH_2-($Si(CH_3)_2$-O)$_n$-$C\mathbf{H}_2$-CH_2-, PDMS macromonomer and brush mixture, m, 4H), 0.09 (-($Si(C\mathbf{H}_3)_2$-O)$_n$-, PDMS macromonomer and brush mixture, s, 68.2H). $Conv_{PDMS} = ([Area(a + a')/68.2] - [Area(d)/1])/[Area(a + a')/68.2] =$ 79%. $n_{bb} = Conv_{PDMS} * \frac{[M]}{[I]} = 79\% * 1125 = 889.$

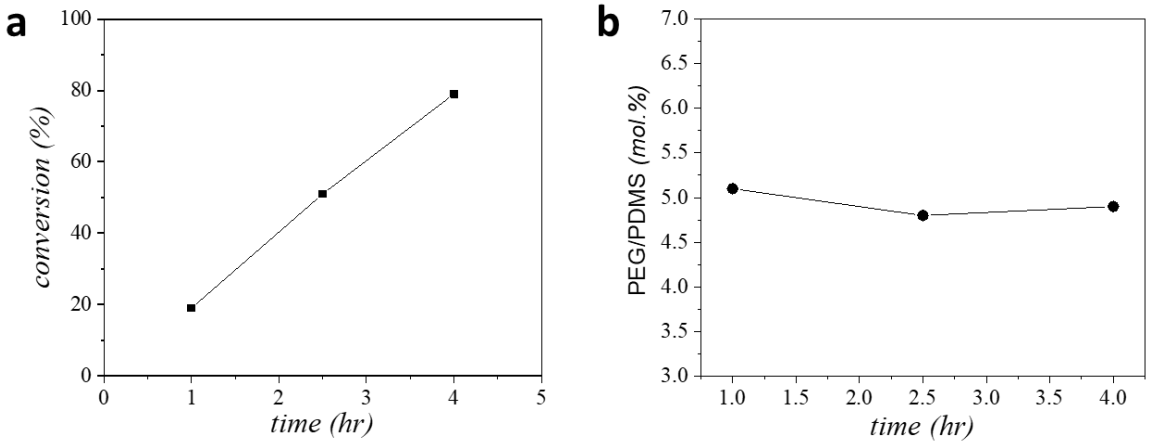

Figure S3. a, Growth kinetics of random polydimethylsiloxane-poly(ethylene glycol) (PDMS-*r*-PEG) copolymer bottlebrushes. **b**, Molar ratio of PEG during copolymerization.

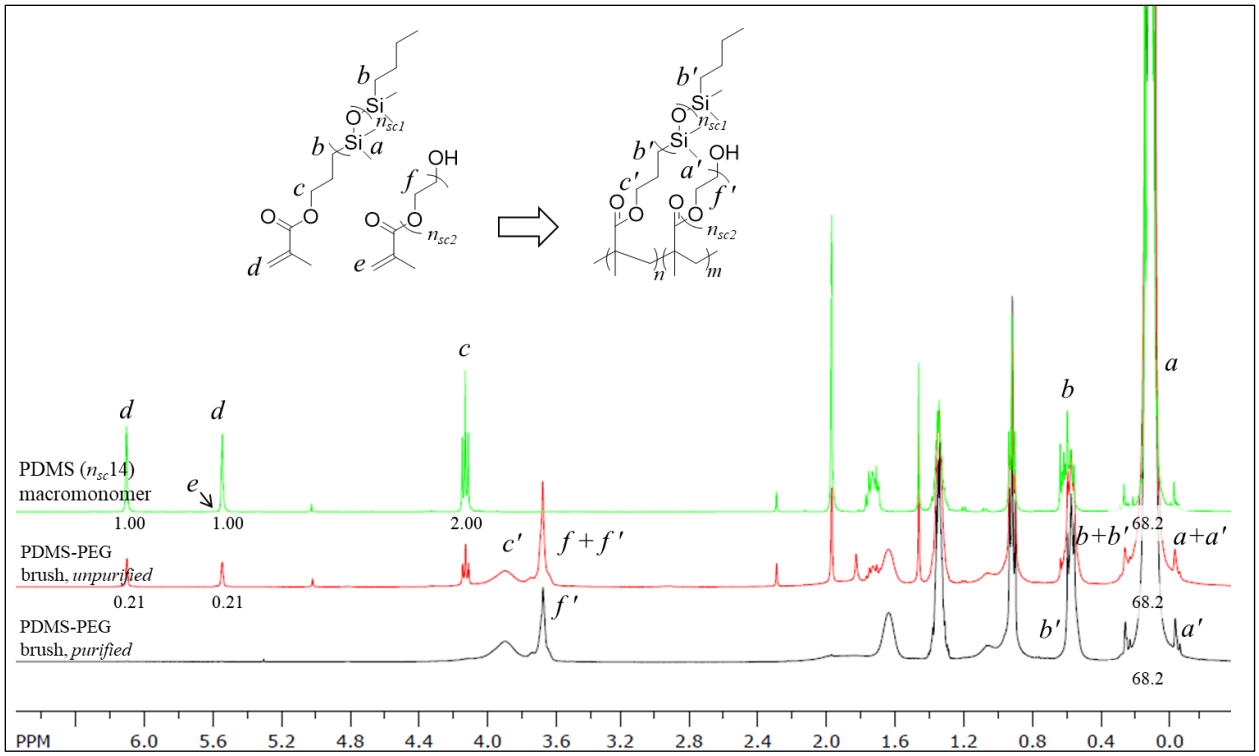

Figure S4. ^{1}H-NMR of random polydimethylsiloxane-poly(ethylene glycol) brushes (PDMS-*r*-PEG, *n*:*m*, 95:5, n_{sc1}: 14, n_{sc2}: 12) at different stages of synthesis (400 MHz, $CDCl_3$): 6.16, 5.57 (CH_2=C(CH_3)C=O, PDMS macromonomer, s, 1H), 4.12 (CO-O**C**H_2-, PDMS macromonomer, t, 2H), 3.91 (CO-O**C**H_2-, PDMS brush, t, 2H), 3.78 (CO-O**C**H_2-, PEG brush, t, 2H), 3.67 (-O**C**$_2$**H**$_4$O-, PEG brush, m, 32H), 0.55 (-CH_2-(Si(CH_3)$_2$-O)$_n$-C**H**$_2$-CH_2-, PDMS macromonomer and brush mixture, m, 4H), 0.09 (-(Si(C**H**$_3$)$_2$-O)$_n$-, PDMS macromonomer and brush mixture, s, 68.2H)

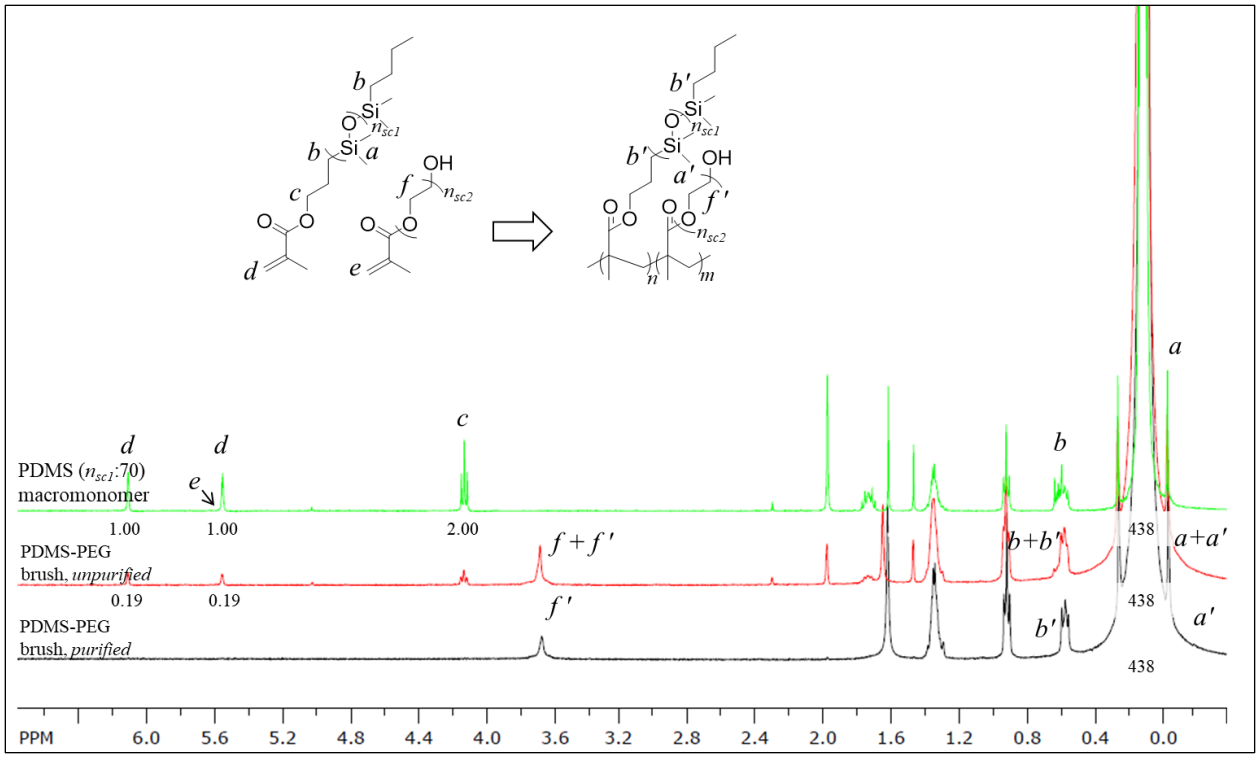

Figure S5. ^{1}H-NMR of random polydimethylsiloxane-poly(ethylene glycol) brushes (PDMS-*r*-PEG, *n*:*m*, 95:5, n_{sc1}: 70, n_{sc2}: 12) at different stages of synthesis (400 MHz, $CDCl_3$): 6.16, 5.57 (CH_2=C(CH_3)C=O, PDMS macromonomer, s, 1H), 4.12 (CO-O**C**H_2-, PDMS macromonomer, t, 2H), 3.91 (CO-O**C**H_2-, PDMS brush, t, 2H), 3.78 (CO-O**C**H_2-, PEG brush, t, 2H), 3.67 (-O**C**$_2H_4$O-, PEG brush, m, 32H), 0.55 (-CH_2-(Si(CH_3)$_2$-O)$_n$-C**H**$_2$-CH_2-, PDMS macromonomer and brush mixture, m, 4H), 0.09 (-(Si(C**H**$_3$)$_2$-O)$_n$-, PDMS macromonomer and bottlebrush mixture, s, 438H). Peak *c′* for brushes with n_{sc1}: 70 do not show on NMR in $CDCl_3$ in contrast to n_{sc3}: 14 brushes. $Conv_{PDMS} = ([Area(a + a')/438] - [Area(d)/1])/[Area(a)/438] = 81\%$. $n_{bb} = Conv_{PDMS} * \frac{[M]}{[I]} = 81\% * 375 = 304$.

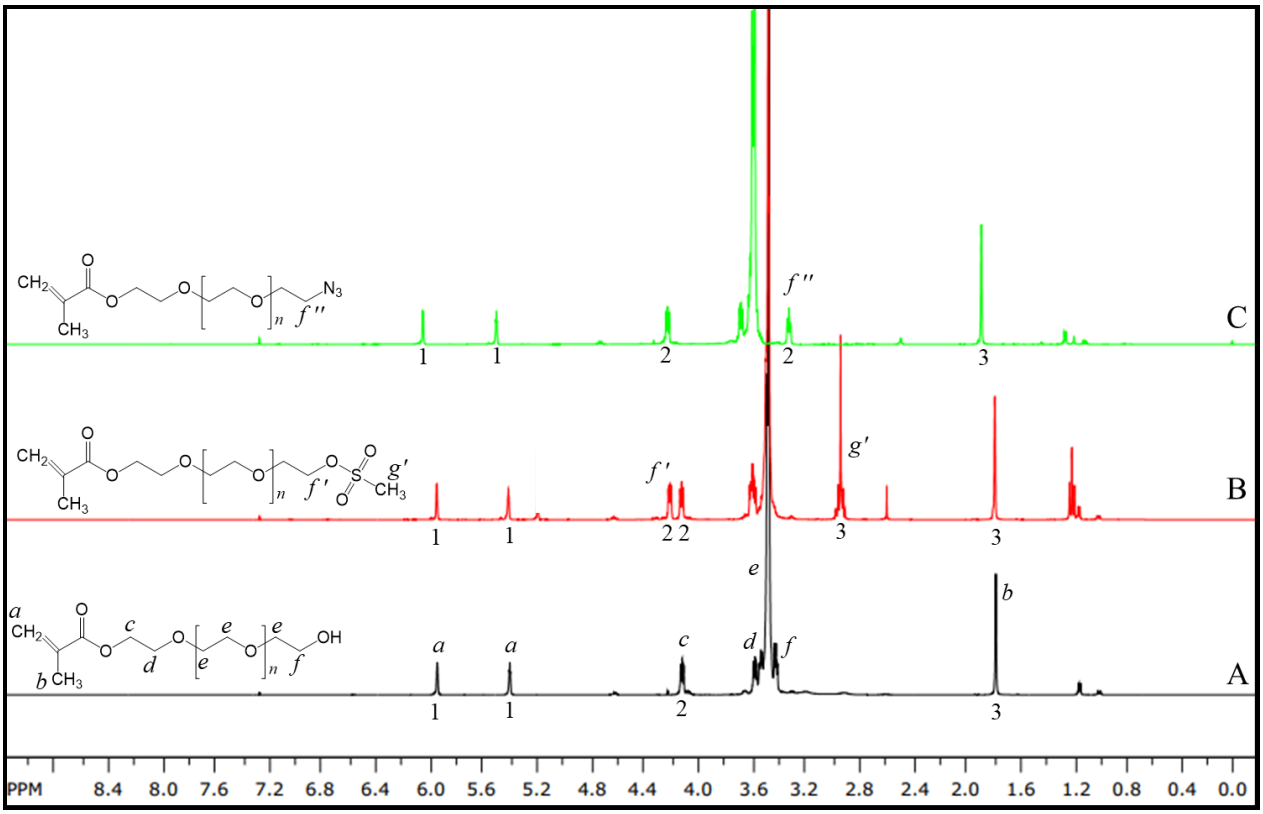

Figure S6. ^{1}H-NMR of poly(ethylene glycol) macromonomer functionalization at different stages. **A**, poly(ethylene glycol) (PEG) macromonomer (400 MHz, $CDCl_3$): 5.98, 5.41 (CH_2=C(CH_3)C=O, s, 1H), 4.15 (CO-OCH_2-, t, 2H), 3.59 (CO-OCH_2-CH_2O-, t, 2H), 3.48 (-OCH_2CH_2O-, m, 32H), 3.42 (-CH_2OH, t, 2H), 1.8 (CH_2=C(CH_3)C=O, s, 3H). **B**, PEG macromonomer after mesylation reaction (400 MHz, $CDCl_3$): 5.98, 5.41 (CH_2=C(CH_3)C=O, s, 1H), 4.22 (-$CH_2OSO_2CH_3$, t, 2H), 4.15 (CO-OCH_2-, t, 2H), 3.59 (CO-OCH_2-CH_2O-, t, 2H), 3.48 (-OCH_2CH_2O-, m, 32H), 2.96 (-$CH_2OSO_2CH_3$, s, 3H), 1.8 (CH_2=C(CH_3)C=O, s, 3H). **C**, azide-terminated PEG macromonomer (400 MHz, $CDCl_3$): 6.05, 5.52 (CH_2=C(CH_3)C=O, s, 1H), 4.21 (CO-OCH_2-, t, 2H), 3.68 (CO-OCH_2-CH_2O-, t, 2H), 3.60 (-OCH_2CH_2O-, m, 32H), 3.37 (-CH_2N_3, t, 2H), 1.90 (CH_2=C(CH_3)C=O, s, 3H).

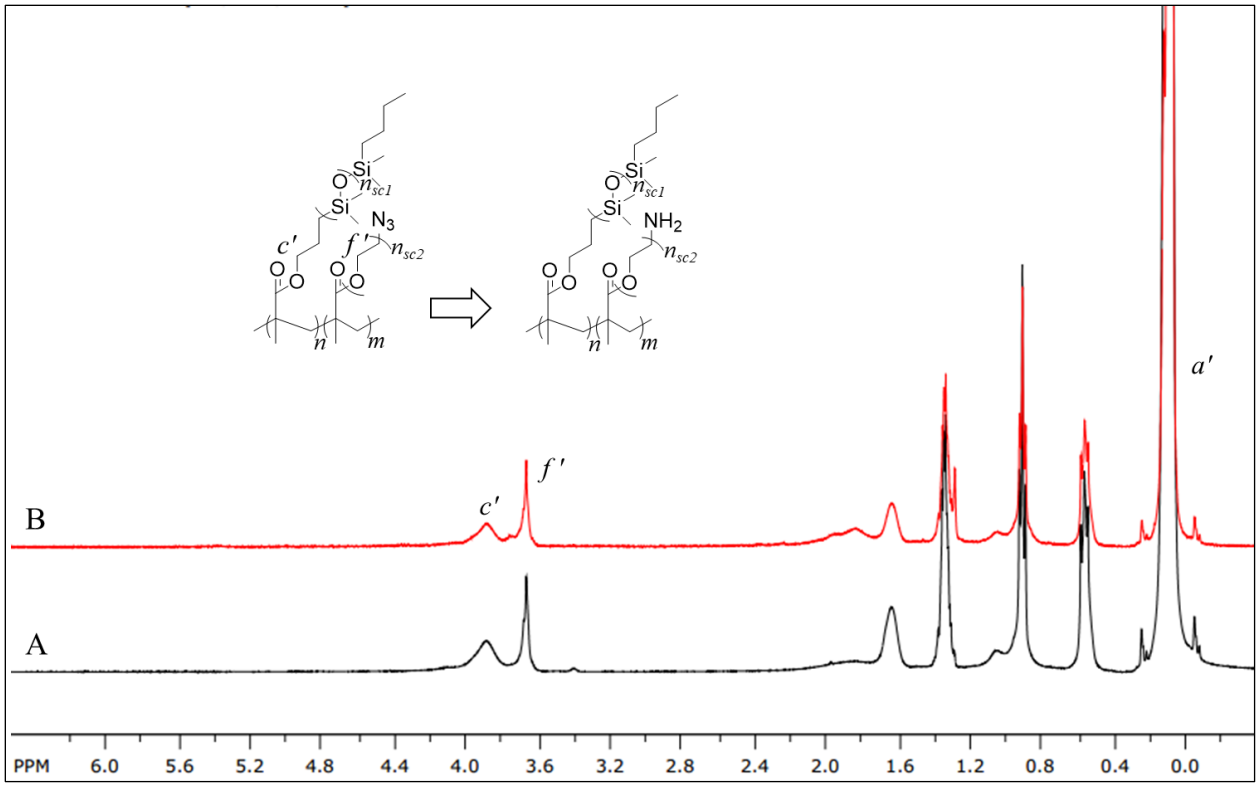

Figure S7. ^{1}H-NMR (400 MHz, $CDCl_3$) of **A**, random polydimethylsiloxane/azide-terminated poly(ethylene glycol) (PDMS-*r*-PEG.N_3), and **B**, random polydimethylsiloxane/amine-terminated poly(ethylene glycol) (PDMS-*r*-PEG.NH_2) bottlebrush copolymer.

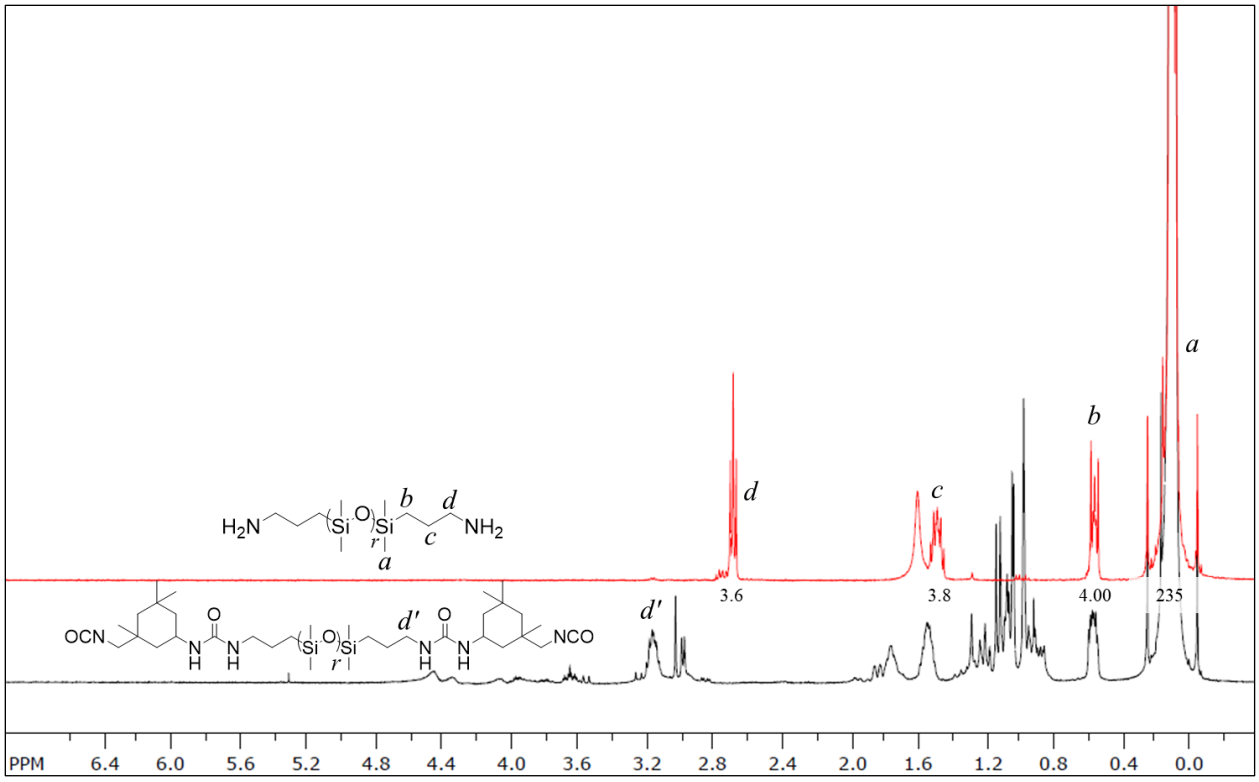

Figure S8. ^{1}H-NMR of polydimethylsiloxane diisocyanate crosslinker (NCO.PDMS.NCO) at different stages of synthesis (400 MHz, $CDCl_3$): 3.18 (-C**H**$_2$-NH$_2$-, crosslinker, t, 2H) 2.69 (-C**H**$_2$-NH$_2$, t, 2H), 0.09 (-(Si(C**H**$_3$)$_2$-O)$_n$ -, s, 235H).

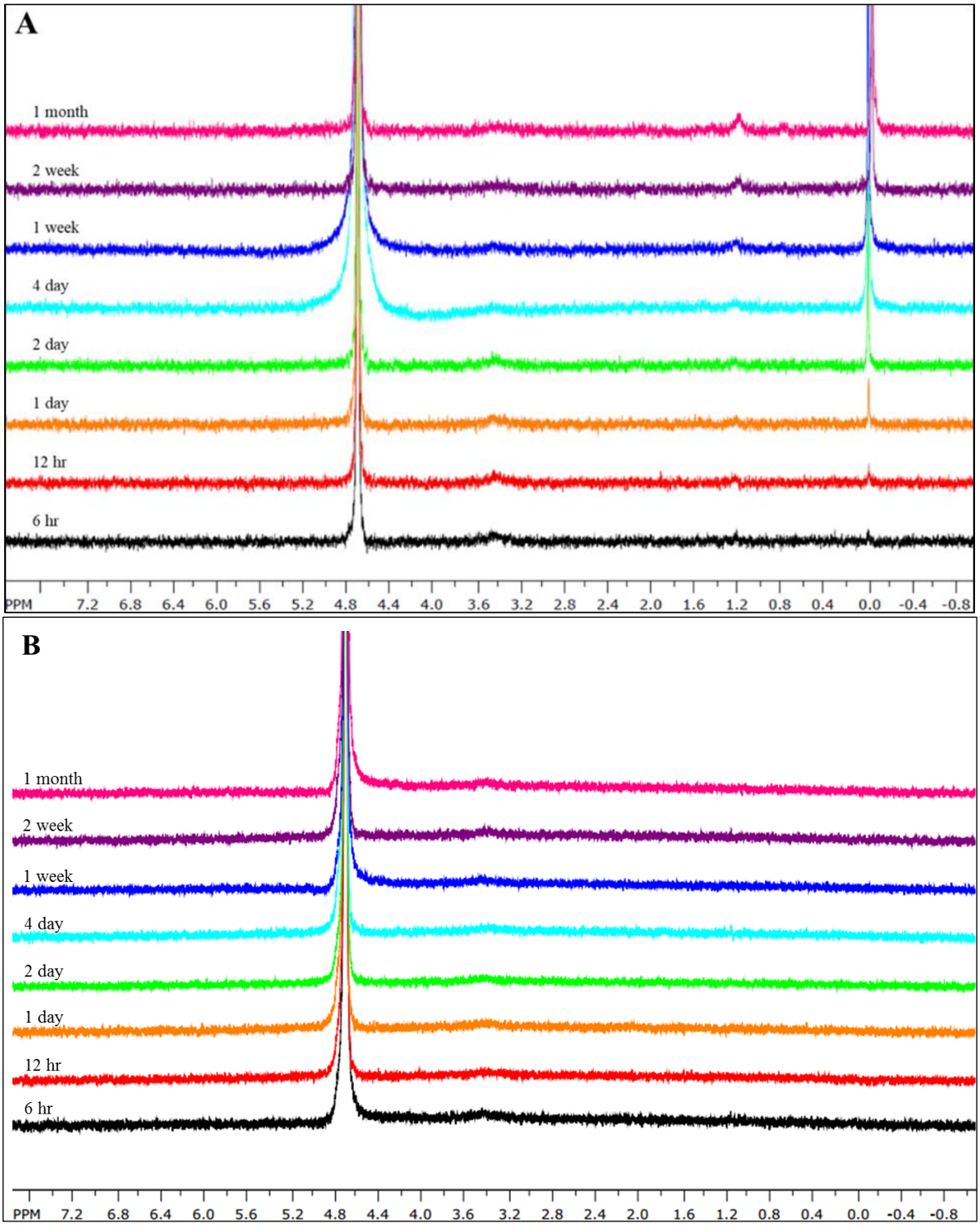

Figure S9. Leachability of injectable elastomer compared to a commercial silicone gel implant into aqueous medium. **A**, Time-resolved ^{1}H-NMR of sol extract from a commercial silicone gel used in breast implants (*Silicone Gel-1* in **Figure S9**) in aqueous medium monitored over one month (400 MHz, $CDCl_3$): 4.70 (Residual H_2O), 1.17, 0.01 (leachable materials). **B**, Time-resolved ^{1}H-NMR of sol extract from a NCO:OH (1:8) injectable elastomer in aqueous medium monitored over a month (400 MHz, D_2O): 4.70 (Residual H_2O); no leachables observed.

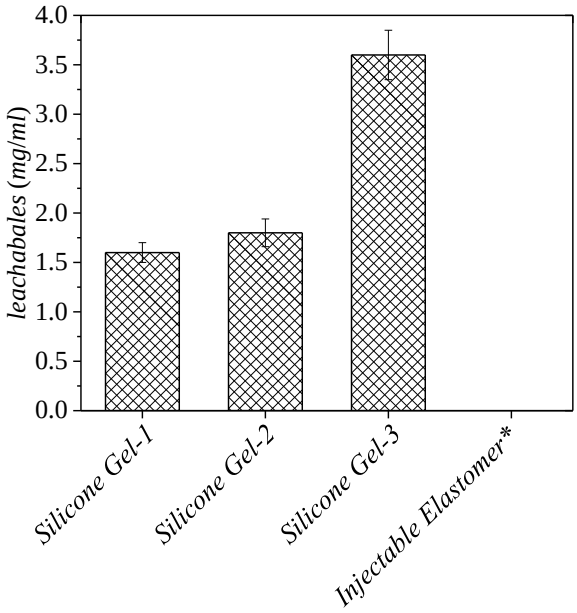

Figure S10. Leachability of three types of commercial silicone gel implants into aqueous medium over a month compared to the injectable elastomer* of NCO:OH (1:8) (400 MHz, $CDCl_3$); data shows mass of leachables from 5 gr gel after one month incubation in 10 ml aqueous medium at room temperature.

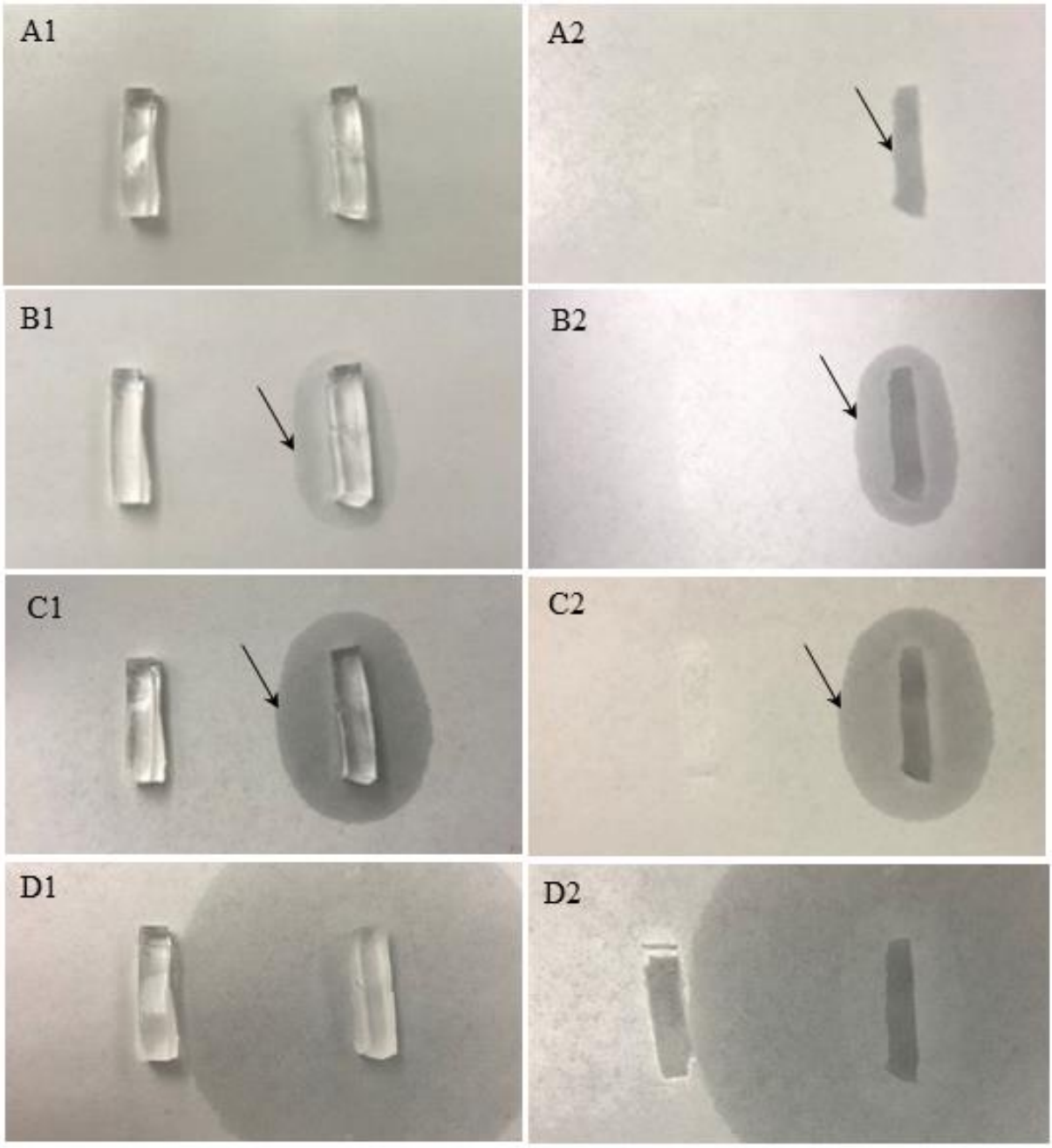

Figure S11. Leachability of a commercial silicone gel used in breast implants (*Silicone Gel-1*) (the right sample in each image) on a paper substrate compared to the injectable elastomer of NCO:OH (1:8) (the left sample in each image). (A1) Front image after 1 hour, (A2) back image after 1 hour, (B1) front image after 1 week, (B2) back image after 1 week, (C1) front image after 1 week, (C2) back image after 1 week, (D1) front image after 1 month, and (D2) back image after 1 month. The leached component from the commercial silicone gel was shown with black arrows.

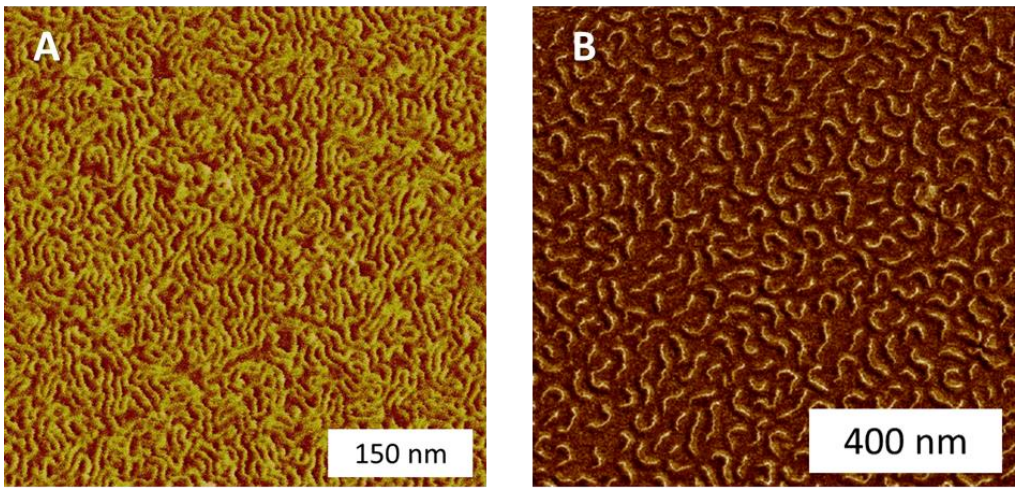

Figure S12. Atomic Force Microscopy of brush polymers. Height micrographs of PDMS-*r*-PEG bottlebrushes deposited on mica by Langmuir-Blodget technique for PDMS: **A**, n_{sc}14, and **B**, n_{sc}70. n_{bb} is determined as L_n/l_0, where L_n is number average measured bottlebrush contour length *via* AFM and l_o= 0.25 nm is the length of bottlebrush backbone monomeric unit. Bottlebrush dispersity, $Đ = M_w/M_n$ is calculated from analysis of > 300 molecules.

Table S1. Molecular characterization of PDMS-*r*-PEG bottlebrushes.

Brush Polymer	n_{bb} **(NMR)**[(1)]	n_{bb} **(AFM)**[(2)]	$Đ$ **(AFM)**[(3)]
n_{sc}14	889	856±55	1.18
n_{sc}70	304	281±35	1.16

[(1)] Number average degree of polymerization of PDMS-*r*-PEG bottlebrush (n_{bb}) determined by ^{1}H-NMR, [(2)] n_{bb}, and [(3)] dispersity ($Đ$) of bottlebrushes determined by AFM (**Figure S8**). n_{bb} was determined by AFM as L_n/l_0, where L_n is number average measured bottlebrush contour length *via* AFM and l_o= 0.25 nm is the length of bottlebrush backbone monomeric unit. Contour length was measured *via* in-house software. Bottlebrush dispersity, $Đ = M_w/M_n$ was calculated based on analysis of ensembles of > 300 molecules to ensure standard deviation of the mean < 10%.

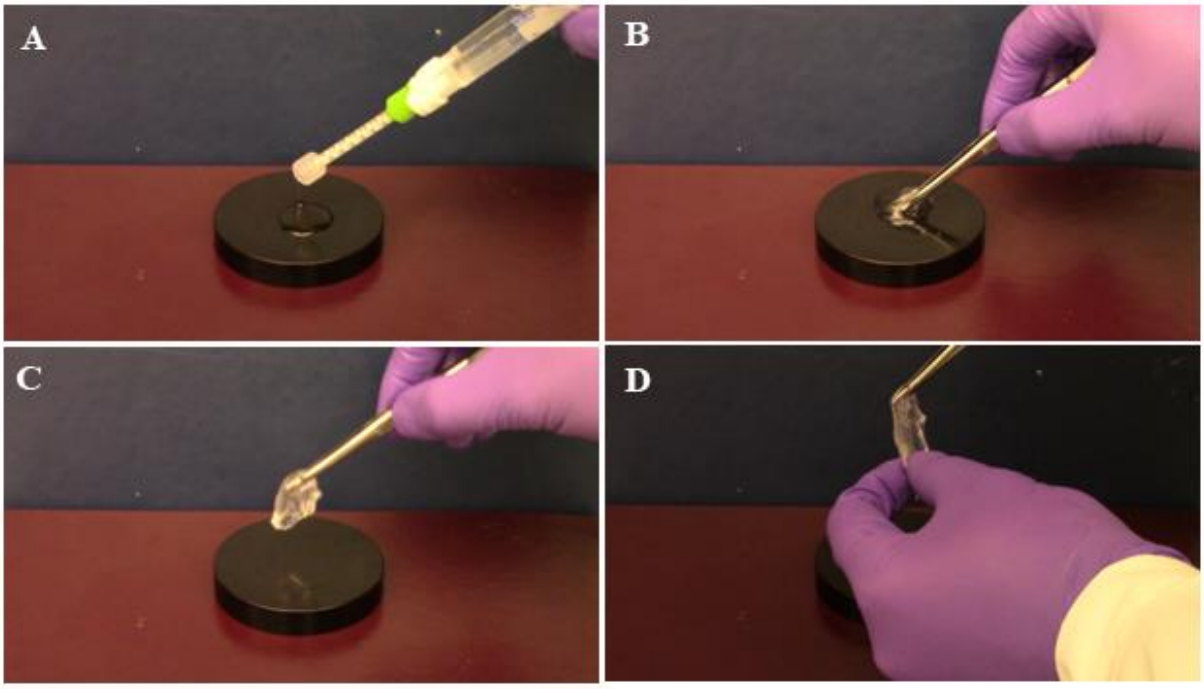

Figure S13. Injectable elastomers: **A**, double-syringe injection, **B**, curing at room temperature, **C**, handling, and **D**, super-soft tissue-mimetic mechanics (Supplementary Video 1).

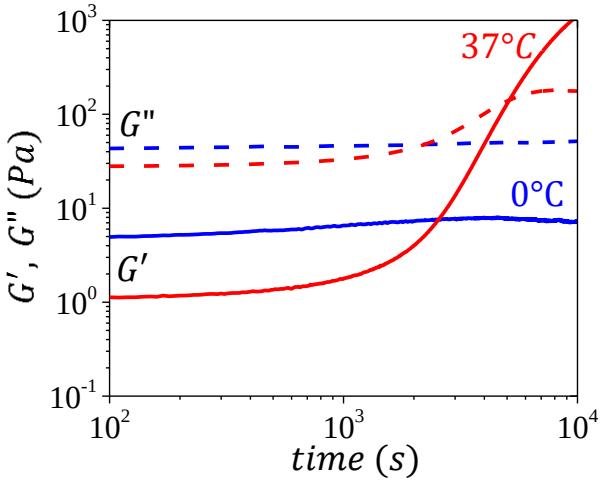

Figure S14. Evolution of elastic (*G'*) and loss modulus (*G"*) as a function of time for injectable elastomers composed of brush chains with hydroxyl groups cured with a macromolecular diisocyanate crosslinker NCO:OH (1:1) at temperatures of 0 and 37ºC. The premixed injectable formulation shows gelation at elevated temperature (37ºC), while it remains fluid at low temperature (0ºC). The formulation remained fluid after 2 months storage at -20ºC, and showed gelation with increasing temperature.

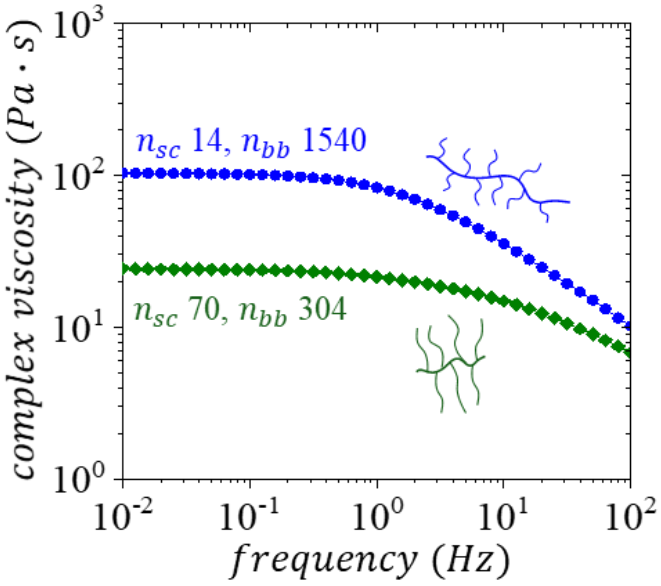

Figure S15. Polydimethylsiloxane (PDMS) bottlebrushes with longer side chains, yet similar molecular weight (M_w = 1,540,000: n_{sc}14, n_{bb}1540 *vs.* M_w = 1,520,000: n_{sc}70, n_{bb}304) possess lower melt viscosity.

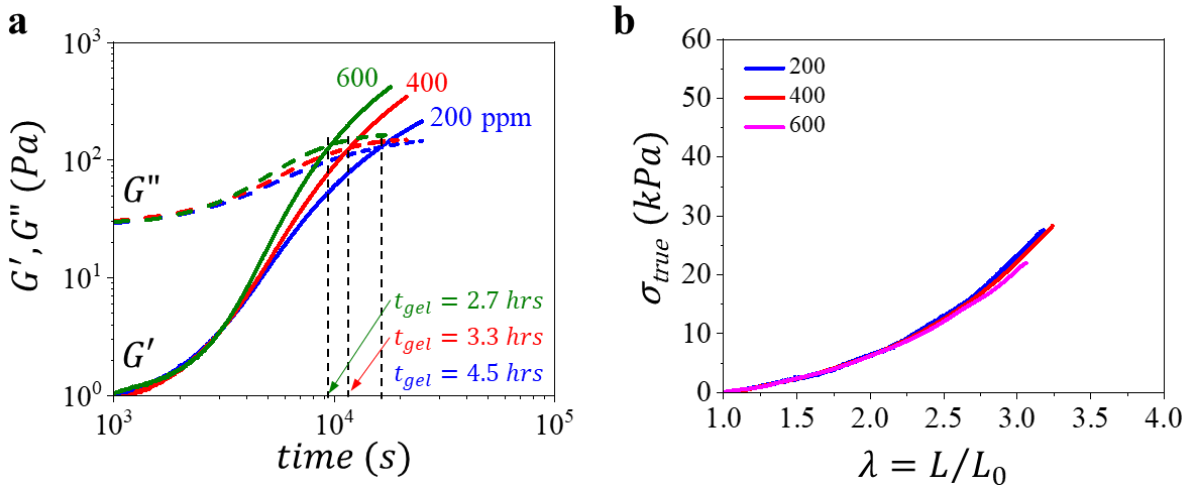

Figure S16. Decoupling gelation time (t_{gel}) and tissue-mimetic mechanics of solvent-free supersoft injectable elastomers: **a**, Evolution of storage (G') and loss (G'') moduli as a function of time for injectable elastomers comprising NCO:OH ratio 1:4 at different content of catalyst (200, 400, and 600 ppm). **b**, True stress-elongation ($\sigma_{true}-\lambda$) curve profiles of the injectable supersoft solvent-free elastomer comprising NCO:OH ratios 1:4 at different content of catalyst (200, 400, and 600 ppm).

Table S2. Structural and mechanical parameters of NCO:OH (1:4) injectable elastomers* comprising different content of catalyst (200, 400, and 600 ppm (Fig. S16b).

Catalyst [1)]	n_{sc} [2)]	n_{bb} [3)]	n_x [4)]	E (kPa) [5)]	β [6)]	E_0 (kPa) [7)]	λ_{max}^{exp} [8)]	λ_{max}^{calc} [9)]
200	14	889	200	4.32	0.104	5.03	3.18	3.10
400	14	889	200	4.35	0.097	5.00	3.24	3.21
600	14	889	200	4.23	0.095	4.85	3.06	3.24

[1)] Catalyst content (DBTDL, ppm). Degrees of polymerization (DP) of [2)] side-chains and [3)] backbone of bottlebrush macromolecules prior to crosslinking determined by ^{1}H-NMR. [4)] Nominal DP of the backbone strand between cross-links. [5)]Structural Young's modulus (G) and [6)] strain-stiffening parameter obtained by fitting stress-strain curves with Equation 1. [7)] Young's modulus from Equation 2. [8)] Experimental elongation at break. [9)] Theoretical elongation at break as $\lambda_{max,calc} = \beta^{-0.5}$. *The gel fraction of injectable elastomers was > 97%.

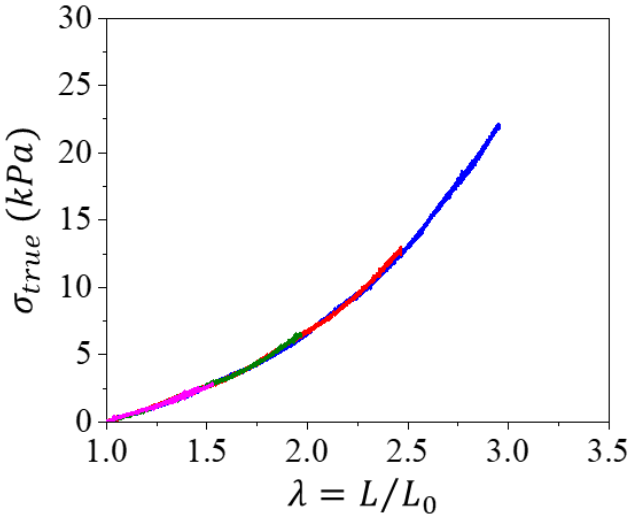

Figure S17. Cyclic loading-unloading curves of injectable elastomer prepared with NCO:OH molar ratio of 1:4 at elongation of λ =1.5 (pink), 2 (green), 2.5 (red), and 3 (blue).

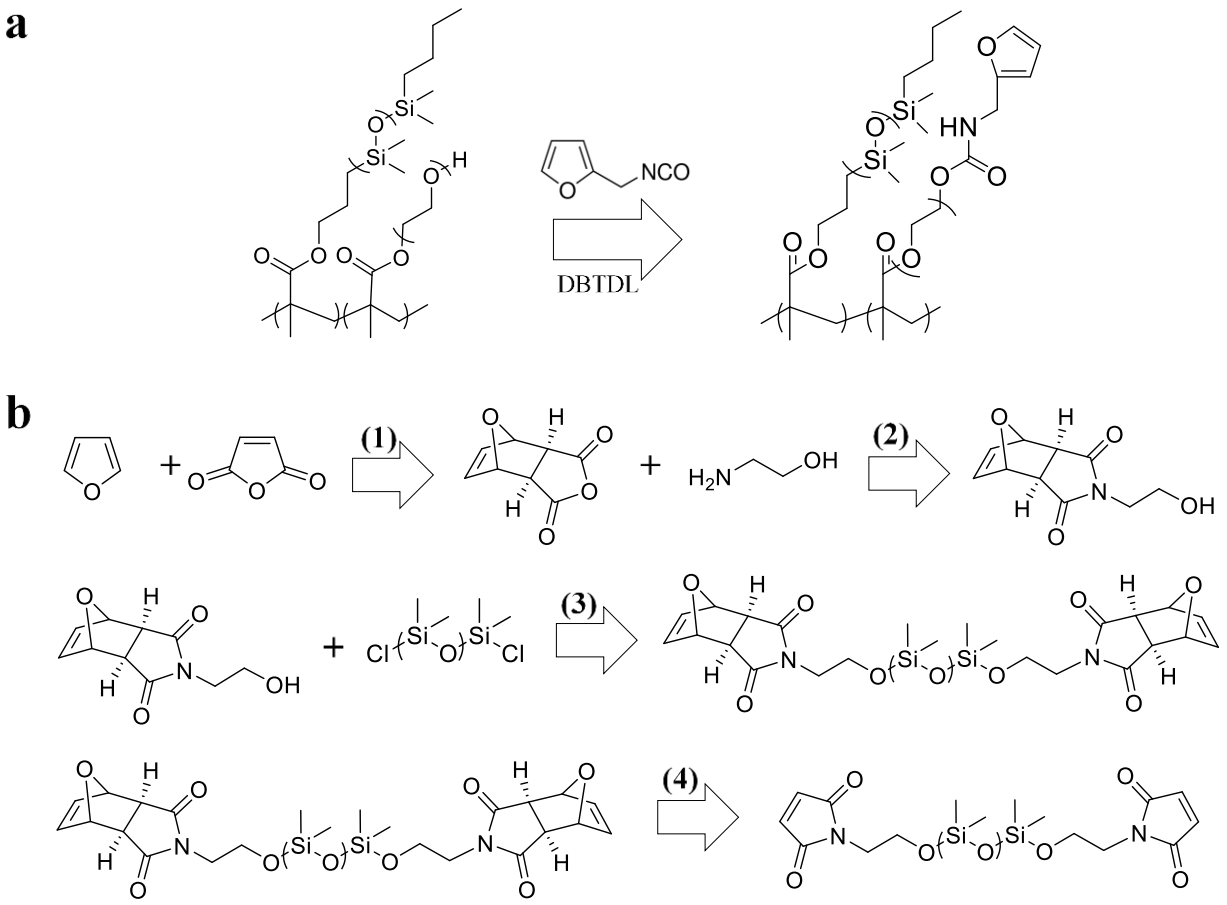

Figure S18. Synthesis of injectable dynamic tissue-mimetic elastomers: **a**, Synthesis of random polydimethylsiloxane-poly(ethylene glycol) (PDMS-*r*-PEG) bottlebrush macromolecules comprising furan moieties. **b**, Synthesis of a linear bifunctional polydimethylsiloxane (PDMS) crosslinker with maleimide moieties: **(1)** synthesis of *exo*-3,6-epoxy-1,2,3,6-tetrahydrophthalic anhydride (furan-protected maleic anhydride), **(2)** synthesis of 2-(2-hydroxyethyl)-3a,4,7,7a-tetrahydro-1H-4,7-epoxyisoindole-1,3(2H)-dione (furan-protected N-(2-hydroxyethyl) maleimide), **(3)** functionalization of chlorine terminated PDMS with furan-protected N-(2-hydroxyethyl) maleimide, **(4)** N-(2-hydroxyethyl) maleimide terminated PDMS as linear bifunctional crosslinker for injectable dynamic tissue-mimetic elastomers (for details of illustrated reactions, please see Methods Section).

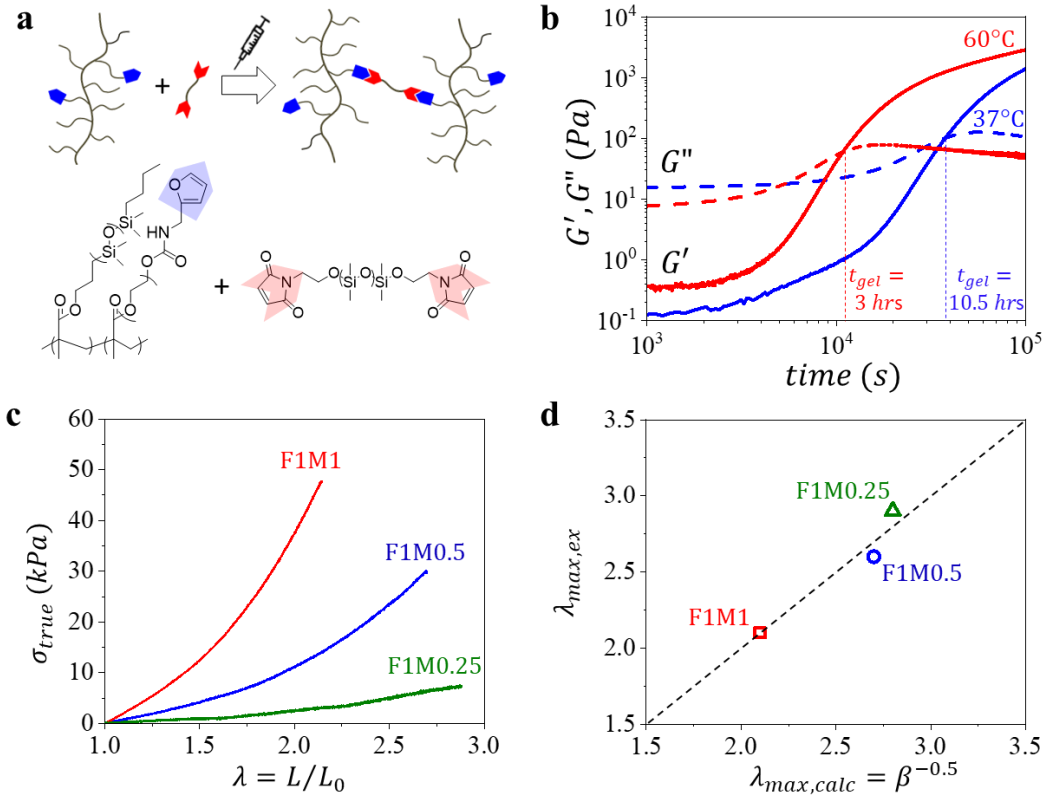

Figure S19. **a**, Injectable reversible tissue-mimetic elastomers composed of random polydimethylsiloxane-poly(ethylene glycol) (PDMS-*r*-PEG) comprising furan (F) moieties with a controlled fraction of a linear bifunctional crosslinker with maleimide (M) moieties (*e.g.*, F1M1 corresponds to 1:1 molar ratio). **b**, Evolution of storage (G') and loss (G'') moduli as a function of time for injectable dynamic elastomer F1M1 at temperatures of 37 and 60ºC. At 37 ºC, the curing time was about 11h, which enables injection of bulky body implants during time-consuming surgery. **c**, True stress-elongation ($\sigma_{true}-\lambda$) curve profiles of the injectable dynamic tissue-mimetic elastomers. **d**, Experimental elongation-at-break ($\lambda_{max,ex}$) demonstrates good agreement with the maximum strand elongation calculated as $\lambda_{max,calc} = R_{max}/\sqrt{\langle R_{in}^2 \rangle} \equiv \beta^{-0.5}$.

Table S3. Structural and mechanical parameters of injectable dynamic elastomers based on Diels-Alder chemistry (Fig. S19c).

F:M [1)]	n_{sc} [2)]	n_{bb} [3)]	n_x [4)]	E (kPa) [5)]	β [6)]	E_0 (kPa) [7)]	λ_{max}^{exp} [8)]	λ_{max}^{calc} [9)]	Gel fraction
F1M1	14	889	50	15.3	0.23	22.3	2.1	2.1	> 98%
F1M0.5	14	889	100	6.3	0.14	7.8	2.7	2.6	> 96%
F1M0.25	14	889	200	1.5	0.12	1.8	2.9	2.8	> 91%

[1)] The ratio of furan (F) moieties on PDMS-*r*-PEG bottlebrushes to maleimide (M) moieties on linear bifunctional crosslinker (*e.g.*, F1M1 corresponds to 1:1 molar ratio). Degrees of polymerization (DP) of [2)] side-chains and [3)] backbone of bottlebrush macromolecules prior to crosslinking determined by ^{1}H-NMR. [4)] Nominal DP of the backbone strand between cross-links. [5)] Structural Young's modulus (G) and [6)] strain-stiffening parameter obtained by fitting stress-strain curves with Equation 1. [7)] Young's modulus from Equation 2. [8)] Experimental elongation at break. [9)] Theoretical elongation at break as $\lambda_{max,calc} = \beta^{-0.5}$.

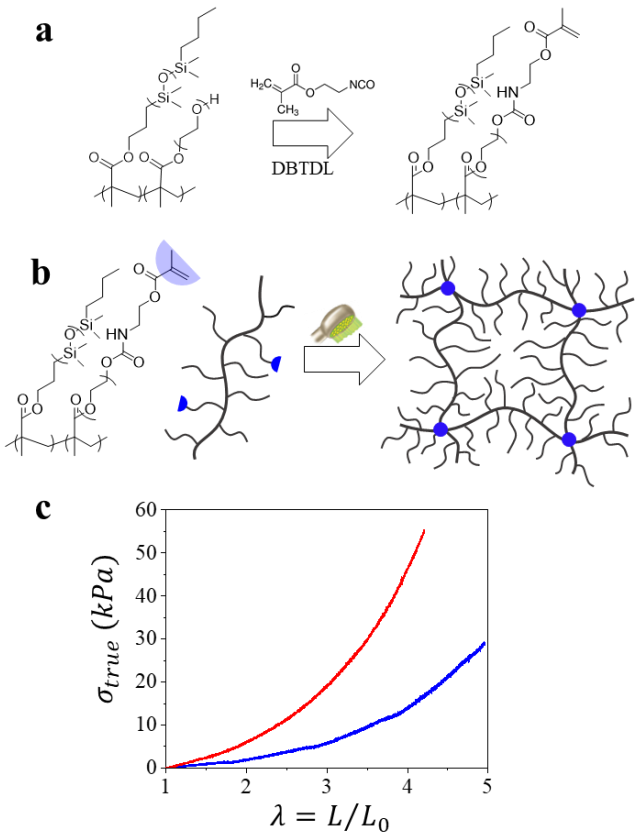

Figure S20. Synthesis of injectable photocurable tissue-mimetic elastomers: **a**, Injectable dynamic tissue-mimetic elastomers composed of random polydimethylsiloxane-poly(ethylene glycol) (PDMS-*r*-PEG) comprising photocurable methacrylate moieties. **b**, True stress-elongation ($\sigma_{true}-\lambda$) curve profiles of the injectable photocurable tissue-mimetic elastomers.

Table S4. Structural and mechanical parameters of injectable photocurable* elastomers (Fig. S20c).

network [1)]	n_{sc} [2)]	n_{bb} [3)]	n_x [4)]	E (*k*Pa) [5)]	β [6)]	E_0 (*k*Pa) [7)]	λ_{max}^{exp} [8)]	λ_{max}^{calc} [9)]	**gel fraction**
Photocure-1.5	14	889	100	4.8	0.06	5.2	4.2	4.1	> 93%
Photocure-3.0	14	889	200	1.7	0.05	1.8	4.9	4.5	> 89%

[1)] Two injectable photocurable tissue-mimetic elastomers are composed of random polydimethylsiloxane-poly(ethylene glycol) (PDMS-*r*-PEG) comprising controlled fraction of PEG macromonomers with chains-end methacrylate moieties at 1.5 and 3 *mol*.%, respectively. Degrees of polymerization (DP) of [2)] side-chains and [3)] backbone of bottlebrush macromolecules prior to crosslinking determined by ^{1}H-NMR. [4)] Nominal DP of the backbone strand between cross-links. [5)]Structural Young's modulus (G) and [6)] strain-stiffening parameter obtained by fitting stress-strain curves with eq 1. [7)] Young's modulus from eq 2. [8)] Experimental elongation at break. [9)] Theoretical elongation at break as $\lambda_{max,calc} = \beta^{-0.5}$.

* The details of conditions of UV procedure is included in the Materials and Methods Section: Functional bottlebrushes were dried with dry N_2 flow until a constant mass was reached. The functionalized brushes were subsequently cured in the presence of diphenyl(2,4,6-trimethylbenzoyl)phosphine oxide/2-hydroxy-2-methylpropiophenone as photo-initiator under N_2 using a UV illumination chamber (365 nm UV lamp, 0.1 mW/cm^{-2}, 10 cm distance).

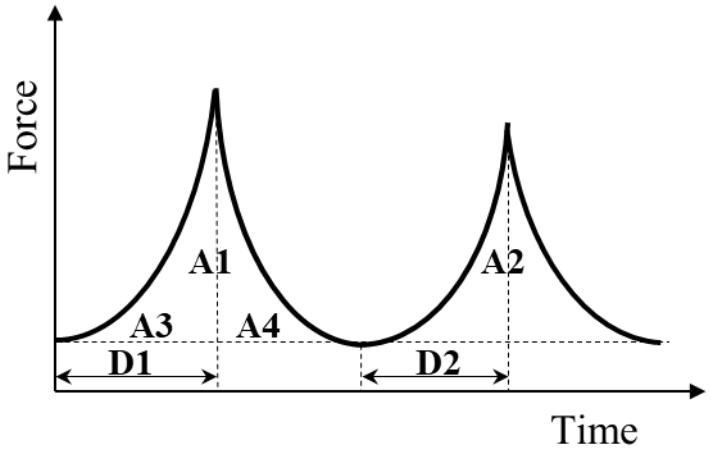

Figure S21. Schematic representation of determining the textural properties including springiness (D2/D1), resilience (A4/A3), and cohesiveness (A2/A1) of injectable non-leaching tissue-mimetic elastomers and commercial implants composed of silicone gel. Texture profile analysis was conducted based on a double compression test.